

Modifications of the metal and support during the deactivation and regeneration of Au/C catalysts for the hydrochlorination of acetylene

Marco Conte,^{*a} Catherine J. Davies,^a David J. Morgan,^a Thomas E. Davies,^a Albert F. Carley,^a Peter Johnston,^b and Graham J. Hutchings ^{*a}

^a *Cardiff Catalysis Institute, School of Chemistry, Cardiff University, Cardiff, CF10 3AT, UK.*

^b *Johnson Matthey Catalysts, Orchard Road, Royston, Herts, SG8 5HE, UK*

E-mail: ConteM1@cardiff.ac.uk, Hutch@cardiff.ac.uk

Abstract

The effect of gold oxidation state and carbon structure on the activity of Au/C catalyst for the hydrochlorination of acetylene was investigated by a combined approach using TPR, XPS and porosimetry determinations. The activity of the catalyst in the synthesis of vinyl chloride monomer was found to be dependent from the presence of Au³⁺ species into the catalyst. However, by preparing catalysts with different Au³⁺ content it was possible to determine the existence of a threshold Au³⁺ amount, beyond which the excess of Au³⁺ was not active for the reaction. This was explained by the existence of active sites at the Au/C interface, and not just by the presence of Au³⁺ species on top of Au nanoparticles, as explained by current models for these catalysts. It was also possible to determine the existence of subset of Au nanoclusters which are not taking part to the reaction, as well as changes in the textural properties of the carbon that can affects its long term reusability.

Keywords: *aqua regia*, gold, carbon, acetylene hydrochlorination, TPR, XPS

1. Introduction

The hydrochlorination of acetylene using HCl is an important industrial route for the manufacture of vinyl chloride monomer (VCM), which is the building block for polyvinyl chloride. It was previously shown that Au/C catalysts can be the best catalysts to carry out this reaction using the direct acetylene hydrochlorination route.¹⁻³ However, the catalyst was found to deactivate, possibly by reduction of Au³⁺ species to Au⁰.^{4,5} When the reaction is carried out in the 120-180 °C temperature range, and by oligomer formation over its surface is the reaction is carried out in the 60-100 °C temperature range.⁶ At present, most VCM is obtained by an oxychlorination reaction using ethylene, O₂ and Cl₂ as reactants.⁷ Due to the current increase in energy costs, coal-based derived feedstocks, like acetylene, are now becoming economically advantageous. Moreover, the industrial catalyst for the direct hydrochlorination reaction, make use of mercuric chloride, a method which efficiency is severely affect by the volatility of this chlorinated salt. These factors prompted us to explore the nature of the active species present over Au/C catalysts with the aim of identifying which of them are responsible for the catalyst activity. Previous studies showed that was possible to regenerate the Au catalyst using Cl₂ and NO.⁶ Alternatively, it was possible to demonstrate that an off-line treatment with *aqua regia* was also an effective regeneration method.⁸ However in all these cases the attention was in the sole change of gold oxidation state without considering possible modifications of the support, as well as postulating Au³⁺ species on top of Au nanoparticles as active sites for the reaction,⁴ without providing clear insights on the possible correlation between the presence of an excess amount of Au³⁺ and the catalytic activity.

This prompted us to investigate the Au/C catalysts by a series of sequential treatments using H₂ as reducing agent and *aqua regia* as oxidizing agent, in order to identify the role of Au³⁺ and Au⁰ in the nanoparticles deposited over the carbon support with respect to catalytic activity. The catalysts were therefore investigated by means on high resolution X-ray photoelectron spectroscopy (XPS) complemented with temperature programmed reduction analysis, being the latter a bulk technique capable to quantify oxidized gold species and changes in the carbon functional groups that could also affect the final reactivity of the catalyst,⁹ by the presence of active gold centers at the Au/C interface. In addition, porosimetry determinations were also carried out, as this proven to be a useful

tool for the determination of carbon textural properties.¹⁰ In fact, an aspect so far neglected in previous studies is the influence of oxidizing acids in the impregnating mixture used to prepare the catalyst that could affect the formation of oxygenated species over the carbon surface¹¹ as well as the pore structure of the carbon,¹² with possible effects on the reusability of this material.

As Au/C catalysts are widely used for reactions other than hydrochlorination e.g. partial oxidation of alcohols^{13,14} and hydrocarbons,^{15,16} we foresee that this work may have a broader application to catalyst design for such reaction.

2. Experimental

2.1 Catalyst preparation

All the catalysts were prepared by a wet impregnation method. The gold precursor, $\text{HAuCl}_4 \cdot x\text{H}_2\text{O}$ (Alfa Aesar, 40 mg, assay 49%) was dissolved in *aqua regia* (3:1 HCl (Fisher, 32%) : HNO_3 (Fisher, 70%) by volume, 5.4 ml) and the solution added dropwise with stirring to the activated carbon support (Norit ROX 0.8) (1.98 g) in order to obtain a catalyst with a final metal loading of 1% wt. Stirring was continued at ambient temperature until NO_x production subsided, approximately 10 minutes. The product was dried for 16 h at 140 °C and used as a catalyst.

Catalyst oxidation was carried out stirring the material in the minimum amount of *aqua regia* to obtain a slurry at room temperature for 10 mins (*i.e.* until NO_x production subsided) followed by drying overnight at 140 °C.

Due to the nature of the catalysts preparation procedure used, wet impregnation,¹⁷ no filtration of the carbon or catalyst washing were carried out, and the metal loading should be considered as equal to the nominal amount of metal impregnated into the support.¹⁸

2.2 Catalytic tests and characterization of the products

Catalysts were tested for acetylene hydrochlorination in a fixed-bed glass microreactor. Acetylene (5 mL min⁻¹, 0.5 bar) and HCl (6 mL min⁻¹, 1 bar) were fed through a mixing vessel

and preheater (70 °C), and further mixed in a N₂ flow (10 mL min⁻¹, 1 bar) *via* calibrated mass flow controllers to a heated glass reactor containing catalyst (200 mg), with a total GHSV of 740 h⁻¹. A reaction temperature of 180 °C was chosen, and blank tests using an empty reactor filled with quartz wool did not reveal any catalytic activity, even at 250 °C with the reactants under these flow conditions, SiC (2 x 2.5g) was used to extend the bed length, above and below the catalyst itself, separated by quartz wool. The pressure of the reactants, HCl, C₂H₂ and N₂, was chosen both for safety reasons and to test the catalyst under mild conditions. The gas phase products were analyzed on-line by GC using a Varian 450GC equipped with a flame ionisation detector (FID). Chromatographic separation and identification of the products was carried out using a Porapak N packed column (6 ft x 1/8" stainless steel).

2.3 Characterization of the catalyst

2.3.1 Temperature programmed reduction

Temperature programmed reduction (TPR) analysis was carried out on a Thermo TPD/R/O 1100 Series instrument equipped with a thermal conductivity detector (TCD), recoding the signal in mV. The sample (100 mg) was heated up to 800 °C at a ramp rate of 5 °C min⁻¹, under a flow of hydrogen (10% in Ar, 20 mL min⁻¹) for the reduction and the oxidations step respectively. Calibration of the detector, and hydrogen consumption, was carried from the integrated TPR (TCD) signal using CuO as a standard¹⁹ (Sigma-Aldrich, 10 mg), subject to the same temperature program used for the Au/C catalysts. The Au³⁺ amount is reported as ratio of Au³⁺ to total Au amount and the absolute amount in mmol (see supplementary data). Peak integration was carried out using SpecView Software. The thermogram was subjected to baseline correction and the area integrated using a cumulative counts algorithm (Fig. S1) CO₂ from decarboxylation reactions was qualitatively identified by heating the carbon in He/H₂ atmosphere and collecting the effluents gases in a saturated solution of BaCl₂·2H₂O, the formation of a BaCO₃ precipitate was detected.

2.3.2 Scanning electron microscopy

Scanning electron microscopy (SEM) and energy dispersive X-ray (EDX) analyses were performed using a Carl Zeiss EVO-40 microscope and Oxford instrument SiLi detector respectively. Samples were mounted on aluminium stubs using adhesive carbon discs. EDX

data were averaged from multiple overscans and spot analysis is considered representative of the sample. SEM was used to analyse the morphology of the samples, while SEM-EDX to determine the chemical composition of the samples.

2.3.2 *X-ray photoelectron spectroscopy*

X-ray photoelectron spectroscopy (XPS) was performed with a Kratos Axis Ultra DLD spectrometer using a monochromatised AlK α X-ray source (120 W) with an analyzer pass energy of 160 eV for survey scans and 40 eV for detailed elemental scans. Binding energies are referenced to the C(1s) binding energy of carbon, taken to be 284.7 eV. As it is well known that cationic Au species can be reduced to the zero-valent state by secondary electron emission samples experience during XPS analysis, the Au(4f) region was recorded at the beginning and end of the analysis.²⁰ The Au³⁺ and Au⁰ amounts are reported as percentage of the total Au amount, and absolute amount in mmol (see supplementary data).

2.3.4 *X-ray powder diffraction*

X-ray powder diffraction spectra (XRPD) were acquired using a X'Pert Panalytical diffractometer operating at 40 kV and 40 mA selecting the Cu K α radiation. Analysis of the spectra was carried out using X'Pert HighScore Plus software. Particle size was determined using the Scherrer equation assuming spherical particles shapes and a K factor of 0.89. The line broadening was determined using a Voigt profile function convoluting the Gaussian and Lorentzian profile part of the reflection peak and the instrumental broadening for the Bragg-Brentano geometry used was estimated to be 0.06° 2 θ .

2.3.5 *Surface area and porosimetry determination*

Surface area and pore size analysis was determined by N₂ adsorption at 77K using a Quantachrome Autosorb AS1. Samples were degassed for a minimum of 24 h at 120 °C before the analysis. Surface areas were evaluated using the BET method and the pore size distribution determined by the Barret-Joyner-Halenda (BJH) method.²¹ The microporous surface area and the external surface area (the area of those pores which are not micropores) was determined by t-plot.

3. Results and discussion

3.1 Correlation between the catalytic activity and gold oxidation state by TPR determinations

In order to verify the effect of oxidized gold species on Au/C catalysts, a catalytic test was carried out with a fresh catalyst (1 % wt Au) and with this material reduced in H₂ atmosphere prior the hydrochlorination reaction (Fig. 1). The fresh catalyst, displayed a conversion-to vinyl chloride monomer of *ca.* 60% with a selectivity virtually of 100% to VCM, with trace amounts (< 0.1%) of 1,2-dichlorethane and chlorinated oligomers only.^{4,6} In contrast, for the catalyst pre-treated in H₂ the activity was limited to only *ca.* 10% conversion.

In order to assess the differences in the Au species for the fresh and the pre-reduced catalyst, temperature programmed reduction (TPR) was used (Fig. 2). It is known that Au³⁺ can reduce in the range of 120-180 °C, and that the catalyst can form oligomers over its surface in the temperature range of 60-100 °C.⁶ However, the analysis carried out to date were all focused in pure changes of oxidation state of the metal. In contrast, by means of TPR we can also probe changes in the carbon support matrix, and therefore to acquire a more accurate picture of the catalyst requirements to be active in case of metal/support interaction. For our catalysts, the fresh Au/C material presents a characteristic reduction band between 230 and 300 °C (with center at 267 °C, Fig. 2 and Fig. S2), which is diagnostic of Au³⁺.²² Comparison of the TCD signal with a standard, permits an estimate of the Au³⁺ amount to be *ca.* 26% of the total Au loading. On the contrary, TPR of the pre-reduced catalyst showed that no Au³⁺ species remained as this reduction band was absent. Control tests with the carbon support with no Au present showed that the activity of the pre-reduced Au/C catalyst was identical to that of the support. This residual activity of the carbon can arise from the presence of trace amounts of K⁺ and Al³⁺ in the carbon matrix, as these metals can display some activity to the hydrochlorination reaction of acetylene.²³ These impurities were identified using SEM-EDX (see ESI Figs. S3 and S4) and the following catalyst atomic composition was determined: C 86.44%, O 9.69%, Na 0.11%, Al 0.05%, Si 0.13%, S 0.22%, Cl 2.34%, K 0.04% and Au 1.04%.

In view of this, and to evaluate systematically the effect of Au³⁺ centres on the catalytic activity, the catalyst was treated off-line with *aqua regia*.⁸ We have previously

demonstrated that a short *aqua regia* treatment of the catalyst can regenerate the catalytic activity without loss of gold metal (as determined by atomic absorption spectroscopy). This was the case also for the Norit carbon support used in the present study, and the catalytic activity was recovered (Fig. 2). More importantly, if the catalyst was subjected to a reduction treatment the catalytic activity was again lost, but if the catalyst was re-oxidized it was able to recover its original activity without any apparent conversion loss when compared to the fresh catalyst.

Using TPR we were able to monitor the amount of Au^{3+} present at each step of the reduction/oxidation cycles, and it is clearly possible to observe that at every oxidation Au^{3+} is restored, and catalytic activity is present, while at each reduction Au^{3+} is absent, and negligible catalytic activity is detected accordingly (Fig. 2). This is an important result, because it shows a high degree of reversibility of the $\text{Au}^{3+}/\text{Au}^0$ system, as well as it implies that the catalyst can support a high number of regeneration by sequential oxidation-reduction, and this could be extremely useful in an industrial context.

An important aspect, in the use of TPR tools for the analysis of the catalysts reported in this study, it is that allows the determination of not just of the gold oxidation state, and quantification of the bulk Au^{3+} amount, but also changes in structural groups present in the carbon matrix. In fact, it should be stressed that activated carbon is not a matrix constituted by carbon only as element, but it has a complex structure characterized by the presence of oxygen in form of carboxylic, ester, ether and lactone groups^{12,24} as well as heteroatoms e.g. phosphorus nitrogen or sulphur, present as phosphates, amine and thiols.²⁵

This was evident by carefully analyzing the TPR profiles, where the oxidation step in presence of *aqua regia* not only regenerated Au^{3+} , but it also effected the oxidation of the carbon support (Fig. 2). From the thermograms (Fig. 2), bands in the range from 450 to 800 °C are assigned to decarboxylation reactions of oxygenated carbon functional groups at the carbon surface, which releases CO and CO₂ with concomitant reduction of oxygenated groups by H₂ in the TPR stream. More specifically, decarboxylation and reduction of oxygenated functional groups reactions in the range of 400-650 °C are attributed to carboxylic acids and carboxylic anhydrides,²⁶ while bands above 650 °C are usually assigned to lactones and phenols.²⁷ Therefore while the pre-treatment of the catalyst in H₂, also reduced the surface carboxylic groups on the carbon, the treatment with *aqua regia*, is capable of inducing carboxyl functionality of the carbon surface as

well as Au³⁺ recovery. This effect on the carbon matrix should be considered a consequence of the presence of HNO₃ in the regeneration step. In fact, this acid is known to induce modifications on the carbon surface inducing oxygenated functional groups,²⁸ as well as changes in the textural properties of the carbon support²⁴ and this was confirmed by XPS porosimetry (this will be discussed subsequently in paragraphs 3.2 and 3.3).

It does worth noting that previous studies on Au/C catalysts for hydrochlorination^{4,29} showed a monotononic deactivation trend ascribed to the reduction of Au³⁺ to Au⁰ and not an activity trend with enhanced activity per time on stream, like the one we are detecting in the current study. On the other hand, for the catalyst reported in the present study, XRPD patterns (Fig. S5) permit an estimate of the mean particles size around 20 nm while in previous cases catalysts having an average particles size in the range of 4-5nm were used, and this could affect the observed trend. Additional tests on the differences in drying temperature that could affect the different particle size and the interface metal/support were also carried out. Two catalysts were prepared using a drying temperature of 110 and 180 °C (Fig. S6). The latter was chosen because the same of the reaction temperature, in order to evaluate if the conversion trend could be affected by the temperature itself. The catalyst dried at 180 °C has a similar trend to those dried at 110 °C, in contrast, the one dried at 140 °C is markedly different with an increase in activity from ca 10% at the beginning of the reaction up to 70% after 5 h of time on stream. It is possible that modifications of the interface Au/C, also induced by the particles size, are responsible of the observed phenomenon. XRPD patterns for the set of catalysts dried at 110, 140 and 180 °C (Fig. S5) showed a particles size distribution centered of < 2 nm, 20 and 3 nm respectively, suggesting that particles size that are too small could not be active for the reaction. On the other hand, previous studies showed that under reaction conditions, the catalyst can be affected by a small, yet detectable, degree of sintering.²⁹

3.1.1 Excess amount of Au³⁺

A further, important aspect in the analysis of the Au³⁺ content, is to assess if there is a threshold beyond which the amount of Au³⁺ is ineffective, or up to which extent the amount of Au³⁺ present in the catalyst can influence the catalytic activity. In fact, while

there is a clear distinction between the reduced Au/C catalysts with no Au³⁺ (which are not active for the reaction), and the oxidized catalyst with a range amount of Au³⁺, (which are active for the reaction), by analyzing the amount of Au³⁺ for the fresh catalyst, the catalyst after first oxidation, and the catalyst after second oxidation (Fig. 2), the Au³⁺ content was *ca.* 26, 36 and 40% respectively. This would suggest that despite Au³⁺ is clearly needed for the reaction, above a give limit excess of Au³⁺ does not increment the activity further. In view of this, we prepared a set of catalysts using a different HCl/HNO₃ ratio in the starting impregnation mixture spanning from 0 to 0.5 HNO₃ volume fraction. In fact in HCl/HNO₃ mixtures is HNO₃ that is responsible for changes in oxidation state of gold, as well as textural properties of the carbon.²⁴ The Au³⁺ content was determined for each catalyst by means of TPR, and compared with the corresponding catalytic activity after 5 h (Fig. 3 and Figs. S7 and S8). Interestingly, a vulcano plot is obtained (Figs. 3 and S7), centred at the *aqua regia* composition (0.25 HNO₃). This shows that if the amount of Au³⁺ increases (in the range 0 to 0.25 HCl/HNO₃) the activity also increases. However, if the amount of Au³⁺ increases further, no actual gain in activity is obtained but rather a decrease in conversion. It should also be stressed that while in this set of experiments at different HCl/HNO₃ ratio, increased Au³⁺ amount was obtained per increased HNO₃ amount, rather than repeated *aqua regia* treatment and done initially. This result, would suggest that the most active catalyst is not necessarily the material with the highest Au³⁺ content, but possibly the material that has Au³⁺ at the appropriate catalyst sites. Thus suggesting the existence of active Au³⁺ sites at the Au/C interface and not just at the surface of Au nanoparticles as previously postulated.⁴

3.2 X-ray photoelectron spectroscopy and particle size distribution

In order to correlate bulk changes of the catalyst structure, with the surface of gold nanoparticles, X-ray photoelectron spectroscopy (XPS) was systematically carried out for all these samples (Fig. 4 and Figs. S9 to S15). It should be noted that where more than one Au species was evident, curve fitting was employed to determine the ratio of each species. As shown in Table 1, the XPS results confirm the TPR measurements and indicate the deactivated catalysts contain Au⁰ only. Similarly, for the active catalysts, the Au³⁺ content was found to follow the same general trend obtained from TPR.

Quantification of the Au³⁺ content reveals a fluctuation between *ca.* 12 and 25% of the overall gold content after regeneration (Tables 1 and S1), however regardless of the overall amount all catalysts are capable of reaching similar conversion values of *ca.* 60%. This result may further indicate that it is not just the presence of Au³⁺ which is responsible for the observed reactivity, but also the location of such species (the Au³⁺ amount from XPS are always lower than those obtained by TPR as the first is a surface method, while the latter a bulk technique). The observed increase in surface oxygen content (Table 2) after each regeneration cycle is a consequence of the oxidising effect of the nitric acid in the *aqua regia* regeneration medium^{24,30} and could be responsible for stabilising the high Au³⁺ oxidation state, particularly as there is no decrease in the surface oxygen content of the reduced samples, together with the absence of any Au³⁺ species.

However, the most important feature of the XPS spectra is possibly that the preparation of these catalysts also forms small metallic gold clusters (hereafter labelled Au⁰-s), the binding energy of which is *ca.* 1 eV higher than the Au(4f) binding energy for the majority of the Au⁰ species^{31,32} (Table 2 and Fig. 4). As we, as well as other researchers²⁰ have previously observed, Au⁺ will also reduce to Au⁰; which is not observed under prolonged X-ray analysis here. However, we consider the Au⁰-s species, to be nothing more than a spectator species, since the reduced catalysts also contain these Au⁰-s nanoclusters and are inactive, although small gold clusters are active for a range of reactions such as CO oxidation.³³

Therefore, considering the XPS and XRD reported in this study, as well as previous work, these data could suggest a particles size range for the particles activity from 5²⁹ to 20 nm.

It should also be underlined that the apparent decrease in Au content detected from XPS analysis is an effect induced by pore changes in the carbon structure by nitric acid,^{16, 17} and therefore gold particles are present also inside the carbon pores and not just at the surface of it. In fact when SEM-EDX was used in view of the major penetration depth of this method a composition close to 1% was detected.

3.3 Textural properties of the Au/C catalysts

To corroborate this experimental results, porosimetry determinations were carried out on an untreated carbon support, a fresh catalyst and a catalyst after oxidation treatment

with *aqua regia*

Adsorption of N₂ resulted in the formation of a type 1 isotherm typical of microporous material (Figs S16 and S17). The narrow pore size distribution curves we obtained are indicative of uniform pore channels in the small mesopore to micropore region. Application of the BJH method shows that the average pore size is in the range 2-3 nm but given the high N₂ uptake at P/P₀ < 0.2 the material likely occupies the microporous to mesoporous range (1-2 nm). The untreated carbon had the lowest surface area of 1153 m²g⁻¹ and the lowest total pore size volume of 0.5318 cm³ g⁻¹ (table 3). Treatment of the catalyst with acid appears to decrease microporosity indicated by the decrease in the S_{mic} and an increase in S_{ext}, which accounts for the external surface area and mesoporous contribution. The microporosity of the catalyst is further decreased by oxidation. It has been shown previously^{10,24} that oxidation and acid treatment of activated carbon results in a decrease in the microporous volume due to the formation of surface oxides at the micropore entrance. It was also shown that strong oxidation can result in a total loss of surface area due to destruction of the pore walls and network.¹² The blocking of micropores as a result of Au addition should also be considered. These factors have been so far fully neglected in the acetylene hydrochlorination reaction, and they suggest that they could be important for the long term usability of this catalyst.

4. Conclusions

It has been confirmed that the activity of Au/C catalysts for the hydrochlorination reaction is invariably associated with the presence of Au³⁺ species, although our data are suggesting that the final activity can be also a consequence of the Au³⁺ location, and not just its concentration, as an excess amount of Au³⁺ does not contribute to the reaction, with important implications in the catalyst design. In addition, the current work provides insights into the active particle size distribution for this catalyst for this reaction, showing that Au nanoclusters are not active for this reaction. This will have important implications with the catalyst preparation targeted to obtain nanoparticles >1 nm and possibly centered in the range 5-20 nm size. The catalysts also showed a large extent of reusability, although changes in textural properties of the carbon were detected.

Acknowledgements

The authors thank Johnson Matthey Plc and World Gold Council for financial support.

References

† Electronic Supplementary Information (ESI) available: catalyst testing, and characterization by XRD, SEM, XPS and porosimetry. See DOI: 10.1039/b000000x/

- 1 G. J. Hutchings, *J. Catal.*, 1985, **96**, 292-295.
- 2 B. Nkosi, N. J. Coville and G. J. Hutchings, *J. Chem. Soc., Chem. Comm.*, 1988, 71-72.
- 3 G. J. Hutchings, *Gold. Bull.*, 1996, **29**, 123-130.
- 4 M. Conte, A. F. Carley, C. Heirene, D. J. Willock, P. Johnston, A. A. Herzing, C. J. Kiely and G. J. Hutchings, *J. Catal.*, 2007, **250**, 231-239.
- 5 B. Nkosi, N. J. Coville, G. J. Hutchings, M. D. Adams, J. Friedl and F. E. Wagner, *J. Catal.*, 1991, **128**, 366-377.
- 6 B. Nkosi, M.D. Adams, N.J. Coville, G.J. Hutchings, *J. Catal.*, 1991, **128**, 378-386.
- 7 I. M. Clegg and R. Hardman, US Patent 5763710, 1998.
- 8 M. Conte, A.F. Carley, G.J. Hutchings, *Catal. Lett.* 124 (2008) 165-167.
- 9 P. Arnoldy, E. M. van OERS, O. S. L. Bruinsma, V. H. J. de Beer, and J. A. Moulijn, *J. Catal.*, 1985, **93**, 231-245.
- 10 N. Zhang, L.-Y. Wang, H. Liu and Q.-K. Cai, *Surf. Interface Anal.*, 2008, **40**, 1190-1194.
- 11 H. Tamon and M. Okazaki, *Carbon*, 1996, **34**, 741-746.
- 12 C. Moreno-Castilla, M. A. Ferro-Garcia, J. P. Joly, I. Bautista-Toledo, F. Carrasco-Marin, and J. Rivera-Utrilla, *Langmuir*, 1996, **11**, 4386-4392.
- 13 A. Corma, A. Leyva-Pérez and M. J. Sabater, *Chem. Rev.*, 2011, **111**, 1657-1712.
- 14 A. Villa, G.M. Veith and L. Prati, *Angew. Chem., Int. Ed.*, 2010, **49**, 4499-4502.
- 15 T. Mallat and A. Baiker, *Chem. Rev.*, 2004, **104**, 3037-3058.
- 16 M. D. Hughes, Y.-J. Xu, P. Jenkins, P. McMorn, P. Landon, D. I. Enache, A. F. Carley, G. A. Attard, G. J. Hutchings, F. King, E. H. Stitt, P. Johnston, K. Griffin and C. J. Kiely, *Nature*, 2005, **437**, 1132-1135.
- 17 J. A. Anderson and M. F. García (Eds.) In: *Supported Metals in Catalysis*, Imperial College Press, London, 2005, p.3.
- 18 B. Delmon, P. Grange, P. Jacobs and G. Poncelet (Eds.) In: *Preparation of Catalysts II*, Elsevier, Amsterdam, 1979, p.235.

- 19 P. Kurr, I. Kasatkin, F. Girgsdies, A. Trunschke, R. Schlögl and T. Ressler, *Appl. Catal. A: Gen.*, 2008, **348**,153–164.
- 20 Y. Fong, B. R. Visser, J. R. Gascooke, B. C. C. Cowie, L. Thomsen, G. F. Metha, M. A. Buntine and H. H. Harris, *Langmuir*, 2011, **27**, 8099–8104.
- 21 E. P. Barrett, L. G. Joyner, P. P. Halenda, *J. Am. Chem. Soc.*, 1951, **73**, 373-380.
- 22 C. Baatz, N. Decker and U. Prüße, *J. Catal.*, 2008, **258**, 165-169.
- 23 K. Shinoda, *Chem. Lett.*, 1975, **4**, 219-220.
- 24 M. Gurrath, T. Kuretzky, H. P. Boehm, L. B. Okhlopkova, A. S. Lisitsyn, V. A. Likholobov, *Carbon*, 2000, **38**, 1241-1255.
- 25 J. K. Brennan, T. J. Bandosz, K. T. Thomson, K. E. Gubbins, *Colloids and Surfaces A: Physicochem. Eng. Aspects*, 2001, **187-188**, 539-568.
- 26 K. Dumbuya, G. Cabailh, R. Lazzari, J. Jupille, L. Ringel, M. Pistor, O. Lytken, H.-P. Steinrück and J.M. Gottfried, *Catal. Today*, 2012, **181**, 20-25.
- 27 Q. Fu, H. Saltsburg and M. Flytzani-Stephanopoulos, *Science*, 2003, **301**, 935-938.
- 28 S. R. de Miguel, O. A. Scelza, M. C. Román-Martínez, C. Salinas-Martínez de Lecea, D. Cazorla-Amorós and A. Linares-Solano, *Appl. Catal. A: Gen.*, 1998, **170**, 93-103.
- 29 M. Conte, A. F. Carley, G. Attard, A. A. Herzing, C. J. Kiely, G. J. Hutchings, *J. Catal.*, 2008, **257**, 190–198.
- 30 J. L. Figueiredo, M. F. R. Pereira, M. M. A. Freitas, J. J. M. Órfão, *Carbon*, 1999, **37**, 1379-1389.
31. C. N. R. Rao, V. Vijayakrishnan, H. N. Aiyer, G. U. Kulkarni, G. N. Subbanna, *J. Phys. Chem.*, 1993, **97**, 11157-11160.
32. T. V. Choudhary, D. W. Goodman, *Top. Catal.*, 2002, **21**, 25-34.
34. A. A. Herzing, C. J. Kiely¹, A. F. Carley, P. Landon, G. J. Hutchings, *Science*, 2008, **321**, 1331-1335.

Tables, pictures and captions

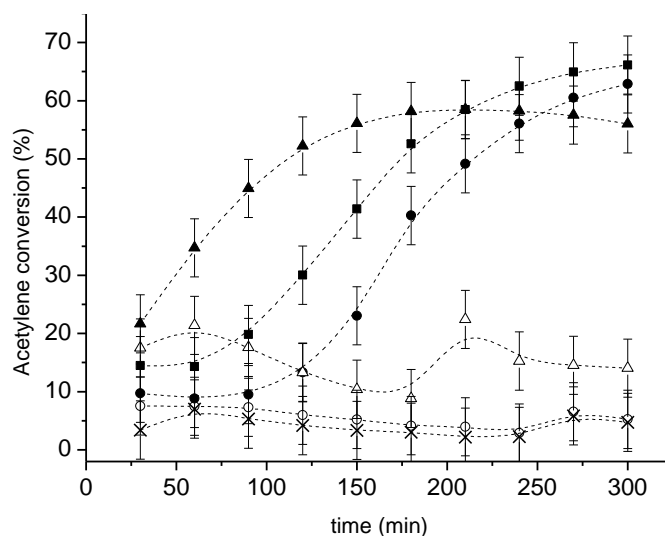


Fig. 1 Acetylene conversion over Au/C (1% wt) catalysts subject to reduction and oxidation cycles, (■) fresh catalyst, (○) reduced catalyst, (●) first catalyst oxidation, (Δ) second catalyst reduction, (▲) second catalyst oxidation, (x) third catalyst reduction.

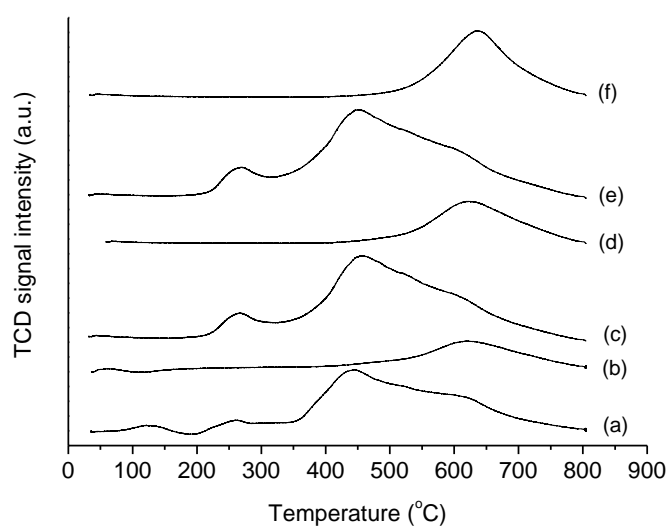


Fig. 2 TPR profiles for Au/C catalysts subject to reduction and oxidation cycles, (a) fresh catalyst, (b) reduced catalyst, (c) first catalyst oxidation, (d) second catalyst reduction, (e) second catalyst oxidation, (f) third catalyst reduction

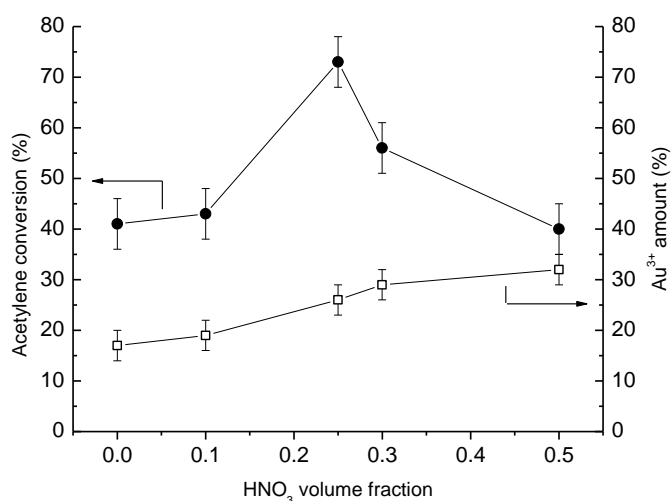


Fig. 3 Conversion (●) after 5 h and Au³⁺ (□) amount for Au/C catalysts containing different amount of Au³⁺. The catalysts were obtained from impregnation using solutions containing different HNO₃ volume fraction in the HCl/HNO₃ mixture.

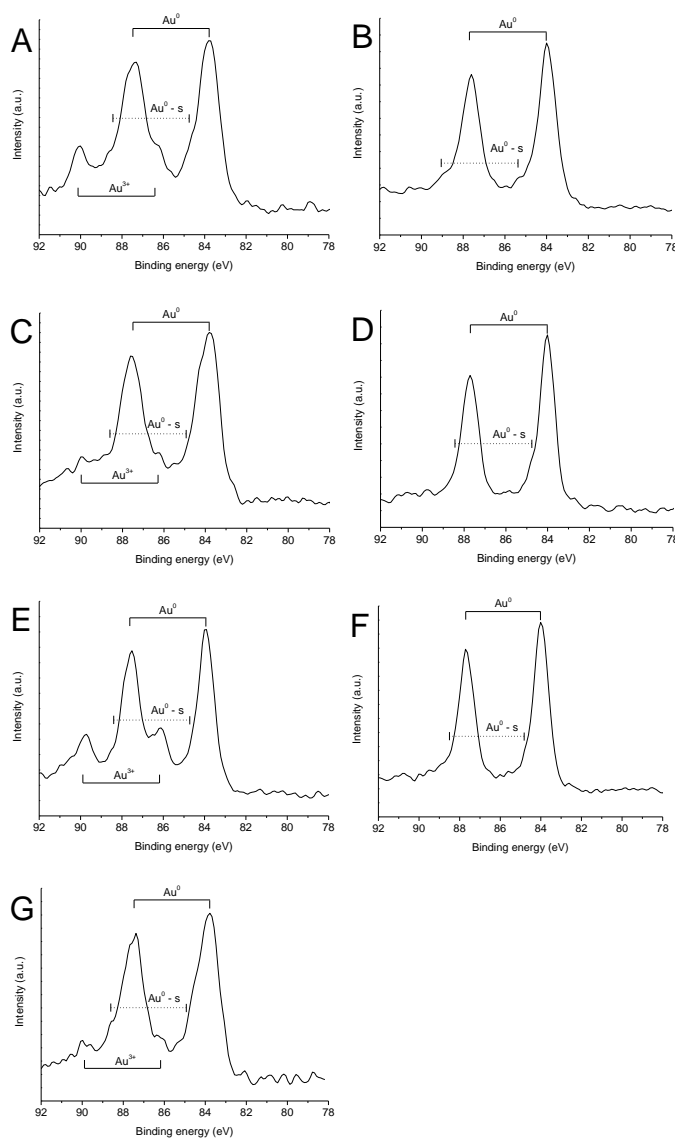


Fig. 4 XPS profiles for Au/C catalysts subject to reduction and oxidation cycles, (A) fresh catalyst, (B) reduced catalyst, (C) first catalyst oxidation, (D) second catalyst reduction, (E) second catalyst oxidation, (F) third catalyst reduction and (G) third catalyst oxidation.

Table 1. Quantification and identification from XPS of Au species over Au/C catalysts subejct to reduction and oxidation cycles.

Catalyst treatment	Au species			Binding energies		
	(%)			(eV)		
	Au ³⁺	Au ⁰	Au ⁰ -s	Au ³⁺	Au ⁰	Au ⁰ -s
fresh catalyst	20.5	65.5	14.0	86.4	83.8	84.9
1 st reduction	0	87.1	12.9	-	83.9	85.4
1 st oxidation	13.1	75.2	11.7	86.3	83.9	85.2
2 nd reduction	0	89.5	10.6	-	84.0	85.1
2 nd oxidation	24.5	67.4	8.1	86.2	83.9	85.1
3 rd reduction	0	90.0	10.0	-	84.0	85.3
3 rd oxidation	12.3	70.2	17.5	86.2	83.8	84.8

Table 2. Surface atomic composition of Au/C catalysts subejct to reduction and oxidation cycles.

Catalyst treatment	Surface atomic composition (%)				
	Au 4f	C 1s	Cl 2p	Na 1s	O 1s
fresh catalyst	0.08	93.30	0.80	0.00	5.81
1 st reduction	0.07	96.21	0.32	0.33	3.06
1 st oxidation	0.06	93.27	1.20	0.00	5.48
2 nd reduction	0.04	97.42	0.13	0.18	2.23
2 nd oxidation	0.06	94.53	1.08	0.40	3.93
3 rd reduction	0.04	97.25	0.13	0.05	2.54
3 rd oxidation	0.04	92.58	1.26	0.08	6.04

Table 3. textural properties of the carbon precursor, the Au/C catalyst and a catalyst oxidized with *aqua regia*.

Sample	S_{BET} (m²g⁻¹)	S_{micro} (m²g⁻¹)	S_{ext} (m²g⁻¹)	V_{Tot} (cm⁻³g⁻¹)	V_{mic} (cm⁻³g⁻¹)	D (nm)
Carbon (Norit ROX0.8)	1153	938	215	0.5318	0.4859	2.2
Au/C fresh	1181	838	343	0.5391	0.4275	2.3
Au/C oxidised	1213	827	385	0.5442	0.4251	2.4